INSTITUTE OF PHYSICS PUBLISHING INVERSE PROBLEMS

Inverse Problems **19** (2003) 1213–1225 PII: S0266-5611(03)61611-4

Uniqueness and convergence of conductivity image reconstruction in magnetic resonance electrical impedance tomography

Yong Jung Kim[1], **Ohin Kwon**[2], **Jin Keun Seo**[3] **and Eung Je Woo**[4]

[1] Impedance Imaging Research Centre, Kyung Hee University, Kyungki 449-701, Korea
[2] Department of Mathematics, Konkuk University, Seoul 143-701, Korea
[3] Department of Mathematics, Yonsei University, Seoul 120-749, Korea
[4] College of Electronics and Information, Kyung Hee University, Kyungki 449-701, Korea

Received 2 April 2003, in final form 7 July 2003
Published 18 September 2003
Online at stacks.iop.org/IP/19/1213

Abstract

Magnetic resonance electrical impedance tomography (MREIT) is a new medical imaging modality providing high resolution conductivity images based on the current injection MRI technique. In contrast to electrical impedance tomography (EIT), the MREIT system utilizes the internal information of current density distribution which plays an important role in eliminating the ill-posedness of the inverse problem in EIT. It has been shown that the J-substitution algorithm in MREIT reconstructs conductivity images with higher spatial resolution. However, fundamental mathematical questions, including the uniqueness of the MREIT problem itself and the convergence of the algorithm, have not yet been answered. This paper provides a rigorous proof of the uniqueness of the MREIT problem and analyses the convergence behaviour of the J-substitution algorithm.

(Some figures in this article are in colour only in the electronic version)

1. Introduction

The primary goal of electrical impedance tomography (EIT) is to provide cross-sectional conductivity images of the human body [3]. When we inject current into an electrically conducting subject through a pair of surface electrodes, the internal current pathway is determined by the conductivity distribution and the shape of the subject. Any local change of the conductivity distribution results in a distortion of the internal current pathway, whose effect is conveyed to boundary voltages. In EIT, we measure the boundary voltages due to multiple injection currents to reconstruct images of the conductivity distribution. However, these boundary voltages are insensitive to a local change of the conductivity distribution and the relation between them is highly nonlinear. EIT images suffer from poor spatial resolution and accuracy due to the ill-posed characteristic of the corresponding inverse problem.

This motivated us to look for a new way of incorporating more information so that we can avoid this ill-posed nature of the inverse problem.

Magnetic resonance electrical impedance tomography (MREIT) was proposed in order to overcome this difficulty in EIT [5, 8, 11, 13, 20, 21]. In MREIT, we note that the injection current produces a magnetic field as well as an electric field. Since we have been relying only on the measured electrical quantities at the boundary of the subject in EIT, the important keyword in transforming the ill-posed problem into a well-posed one is the internal information of the induced magnetic field. Measuring the induced magnetic flux density $\mathbf{B}$ due to the injection current, we can obtain the internal current density distribution $\mathbf{J} = \nabla \times \mathbf{B}/\mu_0$, where μ_0 is the magnetic permeability of free space. This can be done using the magnetic resonance current density imaging (MRCDI) technique [4, 6, 7, 9, 10, 18, 19].

Once the current density $\mathbf{J}$ is acquired, we should effectively utilize it to reconstruct an image of the conductivity distribution. In our previous papers [11, 13], we proposed the J-substitution algorithm which can provide conductivity images with high spatial resolution and accuracy. Experimental verification of the J-substitution algorithm has also been demonstrated in [14] using two different current injections. Although the J-substitution algorithm performs well, it still remains for us to study the uniqueness of the MREIT problem itself and the convergence behaviour of the algorithm.

Let us begin with stating the mathematical model of the MREIT problem. A domain $\Omega \subset \mathbb{R}^n$, $n = 2, 3$, denotes an electrically conducting subject with a conductivity distribution σ. We assume that the domain Ω is bounded and has a connected C^2-boundary. We also assume that the conductivity distribution σ is $C^1(\bar{\Omega})$ and strictly positive $\sigma > 0$. (See remark 2.5 for an extension of the theory for more general cases.)

The injection current g is applied through a pair of electrodes attached at $P, Q \in \partial\Omega$. Assuming that each electrode is a disc with a radius ϵ, we can express the injection current approximately as

$$g(x) = g[\epsilon; P, Q](x) := \begin{cases} \dfrac{1}{\pi\epsilon^2} & \text{if } |x - P| < \epsilon \quad \text{and} \quad x \in \partial\Omega \\ -\dfrac{1}{\pi\epsilon^2} & \text{if } |x - Q| < \epsilon \quad \text{and} \quad x \in \partial\Omega \\ 0 & \text{otherwise.} \end{cases}$$

According to the Maxwell equations, the conductivity σ dictates the relation between g and the corresponding voltage v via the following Neumann boundary value problem:

$$\begin{aligned} &\nabla \cdot (\sigma \nabla v) = 0 && \text{in } \Omega, \\ &\sigma \nabla v \cdot \nu = g && \text{on } \partial\Omega, \end{aligned} \tag{1}$$

where ν is the outward unit normal vector to the boundary. Here, σ and v are unknowns and v depends on σ. For the uniqueness of v, we normalize $v(\xi_0) = 0$, where the choice of $\xi_0 \in \partial\Omega$ is arbitrary as long as it is separated enough from P and Q. The normalization of $v(\xi_0) = 0$ is mathematically equivalent to $\int_{\partial\Omega} v = 0$. In practice, we use a reference or ground electrode at ξ_0 and measure the voltage v with respect to the electrode. Hence, ξ_0 can be regarded as a reference point for voltage measurements.

In MREIT, it is supposed that the magnitude J of the current density vector field $\mathbf{J} = -\sigma\nabla v$ is given. We may take advantage of this additional information, $J := |\mathbf{J}| = \sigma|\nabla v|$, and transform the EIT model in (1) to

$$\begin{aligned} &\nabla \cdot \left(\frac{J}{|\nabla u|} \nabla u \right) = 0, && \text{in } \Omega, \\ &\frac{J}{|\nabla u|} \frac{\partial u}{\partial \nu} = g && \text{on } \partial\Omega, \quad u(\xi_0) = 0, \end{aligned} \tag{2}$$

which has only one unknown function u. Now, the inverse problem of the classical EIT model is converted to the direct problem in (2), where σ can be obtained directly from its solution u by the relation $\sigma = J/|\nabla u|$. However, it must be observed that, if u is a solution of (2), so is cu for any positive constant c. In order to fix this scaling uncertainty, we adopt the normalization of $J(\xi_0)/|\nabla u(\xi_0)| = 1$ that corresponds to the normalization of conductivity values with $\sigma(\xi_0) = 1$. Here, since the choice of ξ_0 is arbitrary, we set it to be the same point for voltage normalization. In practice, we may attach a small amount of material of known conductivity at the point ξ_0 and image the subject including it. Adding this conductivity normalization into (2) together with the positivity of J, we now consider

$$\begin{aligned} &\nabla \cdot \left(\frac{J}{|\nabla u|} \nabla u \right) = 0, \qquad \text{in } \Omega, \\ &\frac{J}{|\nabla u|} \frac{\partial u}{\partial \nu} = g \qquad \text{on } \partial\Omega, \quad u(\xi_0) = 0, \quad \frac{J(\xi_0)}{|\nabla u(\xi_0)|} = 1. \end{aligned} \tag{3}$$

In order to reconstruct $\sigma = J/|\nabla u|$, the solvability of (3) will be the major issue. Unfortunately, it has been proved in a recent paper [12] that the problem (3) with general J has either infinitely many solutions or no solution at all. In practice, the existence is always guaranteed as long as J is the magnitude of the current density, but the non-uniqueness structure raises a serious issue because we do not know whether a reconstructed solution is the true one or not.

The coupled MREIT system was designed in [13] to handle this issue by using two injection currents:

$$g_i(x) = g[\epsilon; P_i, Q](x) \qquad x \in \partial\Omega, \quad i = 1, 2, \tag{4}$$

and it can be expressed as the following coupled system:

$$\begin{aligned} &\nabla \cdot \left(\frac{J_i}{|\nabla u_i|} \nabla u_i \right) = 0, \qquad \text{in } \Omega, \quad i = 1, 2 \\ &\frac{J_1}{|\nabla u_1|} = \frac{J_2}{|\nabla u_2|} \qquad \text{in } \Omega, \\ &\frac{J_i}{|\nabla u_i|} \frac{\partial u_i}{\partial \nu} = g_i \qquad \text{on } \partial\Omega, \quad u_i(\xi_0) = 0, \quad \frac{J(\xi_0)}{|\nabla u_i(\xi_0)|} = 1, \end{aligned} \tag{5}$$

where ξ_0, P_1, P_2 and Q are four different points on $\partial\Omega$. This type of current injection was used in [1]. The second coupling identity in (5) connecting u_1 and u_2 stems from the fact that the variation in σ due to different injection currents is negligible.

The J-substitution algorithm is a natural iterative scheme based on the coupled system (5). Although it performs well in numerical simulations [13] and experimental work [14], the fundamental questions, such as the uniqueness of the coupled MREIT system and the convergence of the algorithm, have not been answered yet. In [12], we only showed that the edges of discontinuity in σ are uniquely decided in two dimensions, while the uniqueness of the smooth part of σ was left open. In this paper, we prove this uniqueness including three-dimensional cases. In section 3, we will explain the convergence behaviour of the J-substitution algorithm.

2. Uniqueness of the MREIT problem

The solution v of the EIT model (1) clearly satisfies the MREIT model (3). Therefore, the existence of the MREIT model is guaranteed as long as the positive function J represents the magnitude of the current density vector field of the EIT model. One of the main difficulties

in obtaining the conductivity distribution is related to the uniqueness issue of the MREIT model (3). In fact, in the process of the transformation from (1) to (3), infinitely many solutions have been introduced and the new model suffers for its non-uniqueness structure. The following proposition manifests in a constructive way how the non-uniqueness of the problem (3) occurs.

Proposition 2.1. *Suppose $u \in C^1(\Omega) \cap H^1(\Omega)$ is a solution of (3). For any $\phi \in C^1(\mathbb{R})$ with $\phi(0) = 0$ and $\phi' > 0$ in $\mathbb{R}$, the following function w is also a solution of (3):*

$$w(x) := \frac{\phi(u(x))}{\phi'(u(\xi_0))} \qquad \text{for } x \in \Omega. \tag{6}$$

Proof. From the definition, $w \in C^1(\Omega)$ and $w(\xi_0) = 0$. Direct computation yields

$$\nabla w(x) = \rho(x)\nabla u(x), \qquad \text{where } \rho(x) := \frac{\phi'(u(x))}{\phi'(u(\xi_0))}. \tag{7}$$

Substituting $x = \xi_0$, we obtain $\nabla w(\xi_0) = \nabla u(\xi_0)$ and

$$\frac{J(\xi_0)}{|\nabla w(\xi_0)|} = \frac{J(\xi_0)}{|\nabla u(\xi_0)|} = 1.$$

Since ϕ is monotonic, $\rho > 0$ and

$$\frac{\nabla w(x)}{|\nabla w(x)|} = \frac{\nabla u(x)}{|\nabla u(x)|}, \qquad x \in \Omega.$$

Hence, w satisfies (3). □

Since there are infinitely many ways to choose the function ϕ in proposition 2.1, there are the same number of solutions of (3). We can easily check that, if u satisfies the EIT model (1), the modified solution w given by (6) also satisfies the same EIT model after replacing σ by

$$\tilde{\sigma} := \frac{\phi'(u(\xi_0))}{\phi'(u(x))}\sigma \qquad \left(= \frac{J}{|\nabla w|}\right).$$

When J is given, we can obtain a conductivity distribution from $\sigma = J/|\nabla u|$. However, from proposition 2.1, we can construct a different solution w, producing another conductivity distribution $\tilde{\sigma} = J/|\nabla w|$. As an example, figure 1 shows two conductivity distributions recovered from two different solutions u and w using the same J.

Now, let us discuss the uniqueness of the coupled MREIT model (5). We assume that σ belongs to the class

$$\Sigma := \{\sigma \in C^1(\bar{\Omega}) : 0 < \sigma < \infty\}.$$

The smoothness condition is used for the simplicity of its analysis and it can be relaxed in various ways as in remark 2.5. We consider a pair $(u_1, u_2) \in H^1(\Omega) \times H^1(\Omega)$ satisfying the following coupled system:

$$\begin{aligned}
&\nabla \cdot \left(\frac{J_i}{|\nabla u_i|}\nabla u_i\right) = 0, \qquad \text{in } \Omega, \quad i = 1, 2 \\
&\frac{J_1}{|\nabla u_1|} = \frac{J_2}{|\nabla u_2|} \in \Sigma, \\
&\frac{J_i}{|\nabla u_i|}\frac{\partial u_i}{\partial \nu} = g_i \qquad \text{on } \partial\Omega, \quad u_i(\xi_0) = 0, \quad \frac{J_i(\xi_0)}{|\nabla u_i(\xi_0)|} = 1, \quad i = 1, 2.
\end{aligned} \tag{8}$$

In the following theorem, we show the desired uniqueness which implies that the conductivity is uniquely decided by two measurements of J_1 and J_2 for both two- and three-dimensional space.

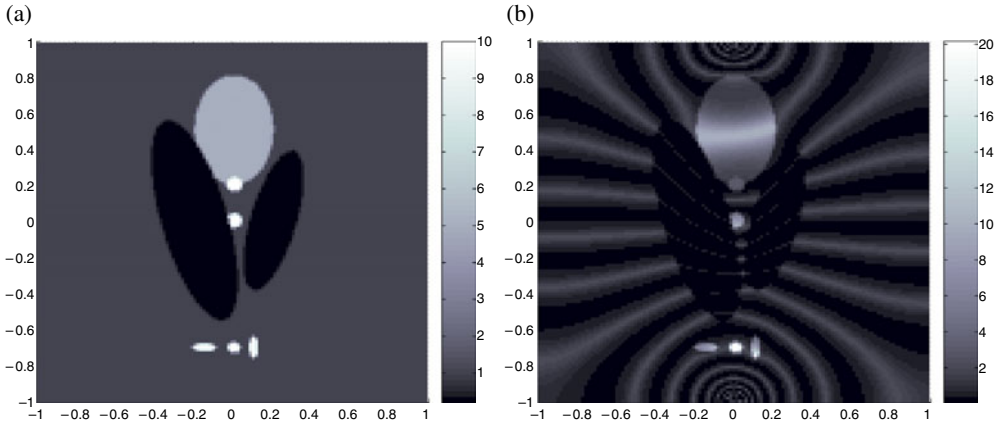

Figure 1. Distribution of (a) $J/|\nabla u|$ and (b) $J/|\nabla w|$, where u and w are two different solutions of (3). Here, $\Omega = (-1, 1) \times (-1, 1)$, $g(x) = \delta(x - (0, 1)) - \delta(x - (0, -1))$, $x \in \partial\Omega$ and ϕ in (6) is chosen so that $\phi'(t) = 2 + 3\sin(400\pi t)/4$ with $\xi_0 = (1, 0)$.

Before describing the theorem, we introduce a couple of lemmas. In proposition 2.1, the gradient vectors of the two solutions w and u have the same direction as in (7). In fact, we show in the following lemma that the gradient vectors of all possible solutions to (3) have the same direction.

Lemma 2.2. *For any two solutions u and $\tilde{u}$ of (3), their gradient vectors ∇u and $\nabla\tilde{u}$ are parallel to each other, i.e.*

$$\frac{\nabla u(x)}{|\nabla u(x)|} = \frac{\nabla\tilde{u}(x)}{|\nabla\tilde{u}(x)|} \qquad \text{for any } x \in \Omega \text{ such that } \nabla u(x) \neq 0, \quad \nabla\tilde{u}(x) \neq 0. \tag{9}$$

Proof. Since u and $\tilde{u}$ have the same Neumann data g, we have

$$\int_\Omega \left(\frac{J}{|\nabla u|}\nabla u - \frac{J}{|\nabla\tilde{u}|}\nabla\tilde{u} \right) \cdot \nabla(u - \tilde{u})\,\mathrm{d}x = \int_{\partial\Omega} (g - g)(u - \tilde{u})\,\mathrm{d}s = 0,$$

which can be written as

$$\int_\Omega \sigma|\nabla u|(|\nabla u| + |\nabla\tilde{u}|)\left(1 - \frac{\nabla u \cdot \nabla\tilde{u}}{|\nabla u||\nabla\tilde{u}|}\right)\mathrm{d}x = 0.$$

Since each factor of the above integrand is non-negative, the whole integrand should be identically zero. Since $\sigma > 0$, $1 - \frac{u(x)\cdot\nabla\tilde{u}(x)}{|\nabla u(x)||\nabla\tilde{u}(x)|} = 0$ if $\nabla u(x) \neq 0$ and $\nabla\tilde{u}(x) \neq 0$. This completes the proof. □

Lemma 2.3. *Let (u_1, u_2) and $(\tilde{u}_1, \tilde{u}_2)$ be solutions of (8). If we set $\sigma = \frac{J_1}{|\nabla u_1|}$, $\tilde{\sigma} = \frac{J_1}{|\nabla\tilde{u}_1|}$ and $\mathbf{J}_j = -\sigma\nabla u_j$, then*

$$\nabla\left(\log\frac{\sigma}{\tilde{\sigma}}\right) \times \mathbf{J}_j = \vec{0} \qquad \text{in } \Omega, \quad j = 1, 2. \tag{10}$$

Proof. Using lemma 2.2, we can easily check that $\tilde{\mathbf{J}}_j (= -\tilde{\sigma}\nabla\tilde{u}_j) = \mathbf{J}_j$, $j = 1, 2$. Since $\nabla \times \nabla u_j = \vec{0}$,

$$\vec{0} = \nabla \times \left(\frac{1}{\sigma}\mathbf{J}_j\right) = \frac{1}{\sigma}(-\nabla\log\sigma \times \mathbf{J}_j + \nabla \times \mathbf{J}_j) \qquad \text{in } \Omega, \tag{11}$$

which leads to $\nabla\log\sigma \times \mathbf{J}_j = \nabla \times \mathbf{J}_j$, and similarly we have $\nabla\log\tilde{\sigma} \times \mathbf{J}_j = \nabla \times \mathbf{J}_j$. By taking the difference of these two identities, (10) is obtained. □

Theorem 2.4. *Let* $(u_1, u_2), (\tilde{u}_1, \tilde{u}_2) \in H^1(\Omega) \times H^1(\Omega)$ *be two pairs of solutions of the system (8). Let* $\sigma = \frac{J_1}{|\nabla u_1|}$ *and* $\tilde{\sigma} = \frac{J_1}{|\nabla \tilde{u}_1|}$. *Then*

$$\sigma = \tilde{\sigma}, \qquad u_1 = \tilde{u}_1, \qquad u_2 = \tilde{u}_2 \qquad \text{in } \Omega. \tag{12}$$

Proof. Set $\mathbf{J}_j = -\sigma \nabla u_j$, $\tilde{\mathbf{J}}_j = -\tilde{\sigma} \nabla \tilde{u}_j$ and $\eta(x) = \log \frac{\sigma(x)}{\tilde{\sigma}(x)}$. Let us begin with proving $\eta = 0$ in Ω for the two-dimensional case. Due to the choice of g_1 and g_2, we have

$$|\nabla u_1(x) \times \nabla u_2(x)| = \begin{vmatrix} \partial_1 u_1(x) & \partial_2 u_1(x) \\ \partial_1 u_2(x) & \partial_2 u_2(x) \end{vmatrix} \neq 0 \qquad \text{for all } x \in \Omega.$$

(See [2, 17] for the proof using level curves.) Hence

$$\mathbf{J}_1(x) \times \mathbf{J}_2(x) = \sigma^2(x) \nabla u_1(x) \times \nabla u_2(x) \neq 0 \qquad \text{for all } x \in \Omega.$$

Lemma 2.3 means that $(-\partial_2 \eta(x), \partial_1 \eta(x)) \cdot \mathbf{J}_j(x) = 0$ for $j = 1, 2$. Since the vectors $\mathbf{J}_1(x)$ and $\mathbf{J}_2(x)$ are linearly independent for all $x \in \Omega$, $\nabla \eta(x) = \vec{0}$ or η is a constant. According to the assumption $\sigma(\xi_0) = 1 = \tilde{\sigma}(\xi_0)$, we have $\eta(\xi_0) = 0$, and therefore $\eta(x) = 0$ for all $x \in \Omega$.

Now, let us prove (12) for the three-dimensional case. (Definitely, the following proof also works for the two-dimensional case.) Suppose $\hat{\Omega}$ is the set of all points x such that $\mathbf{J}_1(x)$ and $\mathbf{J}_2(x)$ are linearly independent:

$$\mathbf{J}_1(x) \times \mathbf{J}_2(x) = \sigma^2(x) \nabla u_1(x) \times \nabla u_2(x) \neq \vec{0} \qquad \text{for all } x \in \hat{\Omega}. \tag{13}$$

Since $\sigma \in C^1(\bar{\Omega})$, $u_j \in C^{1,\alpha}(\Omega)$ for any $0 < \alpha < 1$ and $\hat{\Omega}$ is open. Moreover, we may show that $\bar{\Omega} = \bar{\hat{\Omega}}$. If not, there is an open ball $B \subset \Omega \setminus \hat{\Omega}$ such that $\nabla u_1(x) \times \nabla u_2(x) = \vec{0}$ in B. Let us pick two points $y, z \in B$ such that $u_1(y) \neq u_1(z)$, $\nabla u_1(y) \neq 0$, and $\nabla u_1(z) \neq 0$. Since ∇u_1 and ∇u_2 are parallel in B, u_1 and u_2 have the same level surfaces in B and, in particular, $\{x \in B : u_1(x) = u_1(y)\} = \{x \in B : u_2(x) = u_2(y)\}$ and $\{x \in B : u_1(x) = u_1(z)\} = \{x \in B : u_2(x) = u_2(z)\}$.

Obviously, there exists a closed curve $\gamma \subset \{u_1 = u_1(y)\}$ such that the domain D enclosed by the integral surface passing through γ and the two level surfaces $\{x \in \Omega : u_1(x) = u_1(y)\}$ and $\{x \in \Omega : u_1(x) = u_1(z)\}$ lie in B. Hence, $u_j|_D$ can be viewed as a solution of $\nabla \cdot (\sigma \nabla u_j) = 0$ in D with the special boundary data having $u =$ constant on each of the level surfaces and zero Neumann data on the other boundary. Hence, it is easy to see that $\nabla u_1 = \alpha \nabla u_2$ in D for some constant α. From the unique continuation, $\nabla u_1 = \alpha \nabla u_2$ must hold on the entire domain Ω, which contradicts the boundary conditions g_1 and g_2. Therefore, we obtain $\bar{\Omega} = \bar{\hat{\Omega}}$.

Let $\mathbf{J}_j = (a_j, b_j, c_j)$. From the linear independence between $\mathbf{J}_1$ and $\mathbf{J}_2$, at least one of the following three matrices should be invertible for each $x \in \hat{\Omega}$:

$$A_1(x) := \begin{pmatrix} b_1(x) & c_1(x) \\ b_2(x) & c_2(x) \end{pmatrix}, \qquad A_2(x) := \begin{pmatrix} c_1(x) & a_1(x) \\ c_2(x) & a_2(x) \end{pmatrix},$$
$$A_3(x) := \begin{pmatrix} a_1(x) & b_1(x) \\ a_2(x) & b_2(x) \end{pmatrix}.$$

Moreover, lemma 2.3 implies that

$$\begin{aligned} &A_1 \begin{pmatrix} -\partial_3 \eta \\ \partial_2 \eta \end{pmatrix} = \begin{pmatrix} 0 \\ 0 \end{pmatrix}, \qquad A_2 \begin{pmatrix} -\partial_1 \eta \\ \partial_3 \eta \end{pmatrix} = \begin{pmatrix} 0 \\ 0 \end{pmatrix}, \\ &A_3 \begin{pmatrix} -\partial_2 \eta \\ \partial_1 \eta \end{pmatrix} = \begin{pmatrix} 0 \\ 0 \end{pmatrix} \qquad \text{in } \Omega. \end{aligned} \tag{14}$$

Now, we are ready to prove that $\nabla\eta(x) = \vec{0}$ for all $x \in \hat{\Omega}$. Let x be fixed. Since at least one of the $A_j(x)$ is invertible, without loss of generality we assume that $A_1(x)$ is invertible. According to (14), we have $\partial_2\eta(x) = 0 = \partial_3\eta(x)$ and

$$A_2(x)\begin{pmatrix} -\partial_1\eta(x) \\ 0 \end{pmatrix} = \begin{pmatrix} 0 \\ 0 \end{pmatrix} = A_3(x)\begin{pmatrix} 0 \\ \partial_1\eta(x) \end{pmatrix},$$

which is equivalent to

$$A_1(x)\begin{pmatrix} \partial_1\eta(x) \\ -\partial_1\eta(x) \end{pmatrix} = \begin{pmatrix} 0 \\ 0 \end{pmatrix}.$$

The invertibility of $A_1(x)$ yields $\partial_1\eta(x) = 0$ and we have

$$\nabla\eta(x) = \vec{0} \qquad \text{for all } x \in \hat{\Omega} := \{x \in \Omega : \mathbf{J}_1(x) \times \mathbf{J}_2(x) \neq \vec{0}\}. \tag{15}$$

Hence, $\sigma/\tilde{\sigma}$ is constant for each component of $\hat{\Omega}$. Since $\bar{\Omega} = \bar{\hat{\Omega}}$, the continuity of σ and $\tilde{\sigma}$ leads to $\sigma(x) = c\tilde{\sigma}(x)$ for all $x \in \Omega$ for a constant $c > 0$. Now, the normalization factor $\sigma(\xi_0) = 1 = \tilde{\sigma}(\xi_0)$ implies that $\sigma = \tilde{\sigma}$ in Ω.

Since $\sigma = \tilde{\sigma}$, u_j and $\tilde{u}_j$ are solutions of the same problem (1) with the same Neumann data and, hence, the uniqueness of the Neumann boundary value problem implies $u_j = \tilde{u}_j$. This completes the proof. □

Remark 2.5 (Discontinuous conductivity σ). The smoothness condition on σ can be relaxed in various ways. For example, consider

$$\sigma = \sigma_0 + \sigma_1\chi_{D_1} + \cdots + \sigma_N\chi_{D_N} > 0 \qquad \text{in } \Omega,$$

where D_i are smooth sub-domains of Ω, $\bar{D}_i$ are disjoint and $\sigma_i \in C^1(\bar{D}_i)$. Here, χ_{D_i} is the characteristic function of D_i. Following the lines in the proof of the theorem, we obtain that

$\frac{\sigma}{\tilde{\sigma}}$ is constant in each connected components of $\hat{\Omega} := \{x \in \Omega : \mathbf{J}_1(x) \times \mathbf{J}_2(x) \neq \vec{0}\}$

and the set $\mathcal{T} = \{x \in \Omega : \sigma/\tilde{\sigma}$ is discontinuous at x $\}$ is contained in $\cup_j^N \partial D_j$. Suppose that $\mathcal{T} \neq \emptyset$. Then there exists D_k such that $\partial D_k \subset \mathcal{T}$. Since $\mathbf{J}_j = \tilde{\mathbf{J}}_j$ and $\sigma/\tilde{\sigma}$ has a jump along ∂D_k, it follows from the transmission condition of $\mathbf{J}_j$ and $\tilde{\mathbf{J}}_j$ along the boundary ∂D_k that the vector $\mathbf{J}_j(\tilde{\mathbf{J}}_j)$ on ∂D_k must be normal to ∂D_k. Hence, ∂D_k itself is a level surface of u_j and therefore, according to the maximum principle, u_j is a constant in D_k. Hence, $\nabla u_j = 0$ in the entire Ω, which contradicts the boundary condition g_j.

Remark 2.6 (Injection currents). Theorem 2.4 holds for arbitrary choices of g_1 and g_2 with the same proof for the three-dimensional case. In our experimental studies [11, 14], we attach four electrodes on the surface of the subject, through which we inject currents (or Neumann data).

3. *J*-substitution algorithm and its convergence behaviour

In this section, we first explain the J-substitution algorithm which is a natural iterative scheme of the MREIT system. Then we try to provide some aspects of the algorithm related to its convergence behaviour. Its strong convergence is still left open and we suggest further study on more rigorous convergence analysis.

Using the MREIT model (3), we may design an iterative J-substitution algorithm as follows.

(i) Initial guess $\sigma_0 = 1$.

(ii) For each $n = 0, 1, \ldots,$ solve

$$\nabla \cdot (\sigma_n \nabla u^n) = 0 \qquad \text{in } \Omega,$$
$$\sigma_n \frac{\partial u^n}{\partial \nu} = g \qquad \text{on } \partial\Omega, \quad u(\xi_0) = 0.$$

(iii) Stop the process if $\|J - \sigma_n |\nabla u^n|\|_{L^2(\Omega)} < \epsilon$, where ϵ is a given tolerance.

(iv) Update the conductivity using

$$\sigma_{n+1}(x) = C_n \frac{J(x)}{|\nabla u^n(x)|} \qquad \text{with } C_n = \frac{|\nabla u^n(\xi_0)|}{J(\xi_0)}.$$

The following theorem shows how the sequences of solutions u^n and conductivity distributions σ_n evolve as $n \to \infty$.

Theorem 3.1. *Let u be a solution of (3) and u^n be a sequence of solutions generated by the iterative algorithm. Then, we have*

$$\int_\Omega (\sigma_{n+1} - \sigma)\left\{\left(1 + \frac{\sigma_{n+1}}{\sigma}\right)\frac{J^2}{\sigma_{n+1}^2}\right\} \mathrm{d}x$$
$$= \int_\Omega (\sigma_n - \sigma)\left\{\left(1 + \rho_n \frac{\sigma_{n+1}}{\sigma}\right)\frac{J^2}{\sigma_{n+1}^2}\right\}\left\{\frac{\nabla u^n \cdot (\nabla u^n + \nabla u)}{|\nabla u^n|(|\nabla u^n| + |\nabla u|)}\right\} \mathrm{d}x, \tag{16}$$

where $\rho_n = \frac{|\nabla u(\xi_0)|}{|\nabla u^n(\xi_0)|}$.

Proof. Observing that

$$(\sigma_{n+1}^2 - \sigma^2)|\nabla u^n|^2 = J^2 - \sigma^2 |\nabla u^n|^2 = \sigma^2(|\nabla u|^2 - |\nabla u^n|^2),$$

we obtain

$$\int_\Omega \frac{(\sigma_{n+1}^2 - \sigma^2)}{\sigma} |\nabla u^n|^2 \,\mathrm{d}x = \int_\Omega \sigma\,(|\nabla u|^2 - |\nabla u^n|^2)\,\mathrm{d}x. \tag{17}$$

The right-hand side of the above identity can be written as

$$\int_\Omega \sigma\,(|\nabla u|^2 - |\nabla u^n|^2)\,\mathrm{d}x = \int_\Omega (\sigma_n - \sigma)\nabla u^n \cdot (\nabla u^n + \nabla u)\,\mathrm{d}x$$
$$+ \int_\Omega (\sigma \nabla u - \sigma_n \nabla u^n) \cdot \nabla (u - u^n)\,\mathrm{d}x$$
$$= \int_\Omega (\sigma_n - \sigma)\nabla u^n \cdot (\nabla u^n + \nabla u)\,\mathrm{d}x$$

where we use

$$\int_\Omega (\sigma \nabla u - \sigma_n \nabla u^n) \cdot \nabla (u - u^n)\,\mathrm{d}x = \int_{\partial\Omega} (g - g)(u - u^n)\,\mathrm{d}s = 0.$$

Hence, using $\sigma_{n+1}(x) = C_n \frac{J(x)}{|\nabla u^n(x)|}$, (17) becomes

$$C_n^2 \int_\Omega (\sigma_{n+1} - \sigma)\left\{\left(1 + \frac{\sigma_{n+1}}{\sigma}\right)\frac{J^2}{\sigma_{n+1}^2}\right\} \mathrm{d}x = \int_\Omega (\sigma_n - \sigma)\nabla u^n \cdot (\nabla u^n + \nabla u)\,\mathrm{d}x. \tag{18}$$

Since

$$|\nabla u^n|(|\nabla u^n| + |\nabla u|) = C_n \frac{J}{\sigma_{n+1}}\left(C_n \frac{J}{\sigma_{n+1}} + C\frac{J}{\sigma}\right) = C_n^2\left(1 + \rho_n \frac{\sigma_{n+1}}{\sigma}\right)\frac{J^2}{\sigma_{n+1}^2},$$

the right side of (18) is equal to

$$C_n^2 \int_\Omega (\sigma_n - \sigma)\left\{\left(1 + \rho_n \frac{\sigma_{n+1}}{\sigma}\right)\frac{J^2}{\sigma_{n+1}^2}\right\}\left\{\frac{\nabla u^n \cdot (\nabla u^n + \nabla u)}{|\nabla u^n|(|\nabla u^n| + |\nabla u|)}\right\} \mathrm{d}x.$$

This completes the proof. □

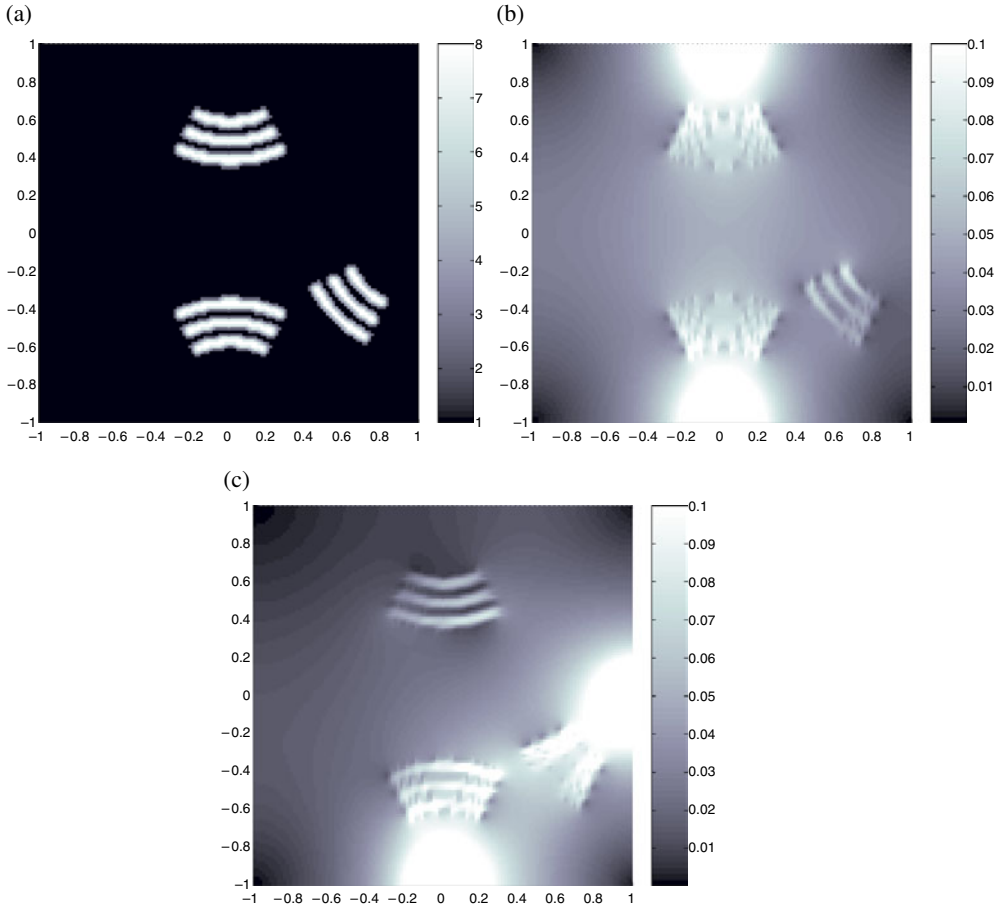

Figure 2. (a) True conductivity distribution to be reconstructed. Distributions of current density in $\Omega = (-1, 1) \times (-1, 1)$: (b) J_1 and (c) J_2 due to $g_1(x) = \delta(x - (0, 1)) - \delta(x - (0, -1))$ and $g_2 = \delta(x - (1, 0)) - \delta(x - (0, -1))$ for $x \in \partial\Omega$, respectively.

Remark 3.2. Note that

$$\frac{|\nabla u^n \cdot (\nabla u^n + \nabla u)|}{|\nabla u^n|(|\nabla u^n| + |\nabla u|)} \leqslant 1$$

and the equality holds only if ∇u and ∇u^n are parallel. Roughly speaking, the effect of the updating process disappears as soon as ∇u^n becomes parallel to ∇u. The sequence obtained by the iterative method may not converge to the true solution u. Instead, it may converge to another solution, which has the same equipotential lines as the true solution.

Since a solution to the MREIT model (3) is not unique, we cannot expect the sequence σ_n generated by the numerical algorithm based on this model to reconstruct σ. Even if it converges, it may show a wrong conductivity. Figure 2(a) shows a true conductivity distribution to be imaged. If we use only one injection current shown in figure 2(b), the iterative algorithm reconstructs the conductivity image shown in figure 3(a). We can clearly observe errors in the reconstructed image. For the numerical simulation, we used the forward solver described in [15].

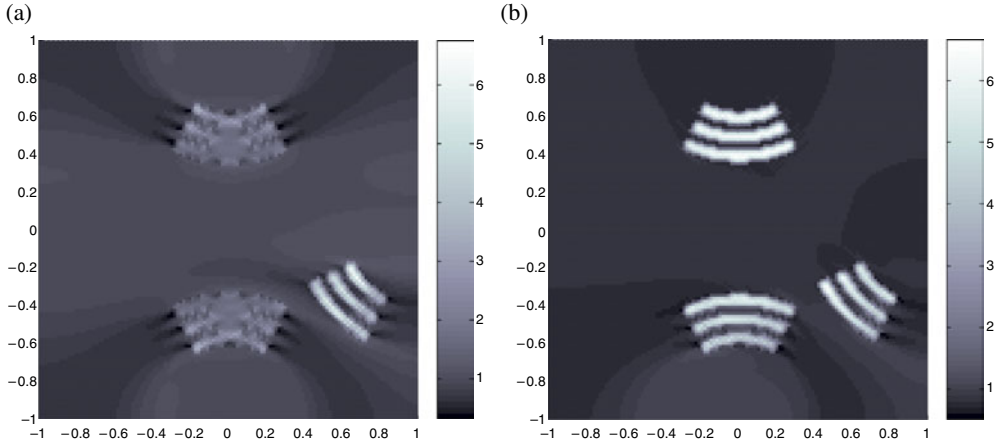

Figure 3. Reconstructed conductivity image using (a) one injection current g_1 and (b) two injection currents g_1, g_2 after 20 iterations.

Now, we consider an iterative method based on the coupled MREIT system (5). Since the conductivity should be given by $\sigma = J_1/|\nabla u_1| = J_2/|\nabla u_2|$, we can easily design the following iterative scheme updating u_1, u_2 and σ.

(i) Initial guess $\sigma_0 = 1$.
(ii) For each $n = 0, 1, \ldots,$ solve

$$\nabla \cdot (\sigma_n \nabla u_1^n) = 0 \qquad \text{in } \Omega$$
$$\sigma_n \frac{\partial u_1^n}{\partial \nu} = g_1 \qquad \text{on } \partial\Omega, \quad u_1^n(\xi_0) = 0.$$

(iii) Update the conductivity using

$$\sigma_{n+1/2}(x) = C_n \frac{J_1(x)}{|\nabla u_1^n(x)|} \qquad \text{with } C_n = \frac{|\nabla u_1^n(\xi_0)|}{J_1(\xi_0)}.$$

(iv) Solve

$$\nabla \cdot (\sigma_{n+1/2} \nabla u_2^{n+1/2}) = 0 \qquad \text{in } \Omega$$
$$\sigma_{n+1/2} \frac{\partial u_2^{n+1/2}}{\partial \nu} = g_2 \qquad \text{on } \partial\Omega, \quad u_2^{n+1/2}(\xi_0) = 0.$$

(v) Stop the process if $\|J_2 - \sigma_{n+1/2}|\nabla u_2^{n+1/2}|\|_{L^2(\Omega)} < \epsilon$, where ϵ is a given tolerance.
(vi) Update the conductivity using

$$\sigma_{n+1}(x) = C_{n+1/2} \frac{J_2(x)}{|\nabla u_2^{n+1/2}(x)|} \qquad \text{with } C_{n+1/2} = \frac{|\nabla u_2^{n+1/2}(\xi_0)|}{J_2(\xi_0)}.$$

The following is clear from theorem 3.1.

Corollary 3.3. *Let a pair (u_1, u_2) be the unique solution of (5) and u_1^n, $u_2^{n+1/2}$ be the sequences generated by the iterative J-substitution algorithm. Then*

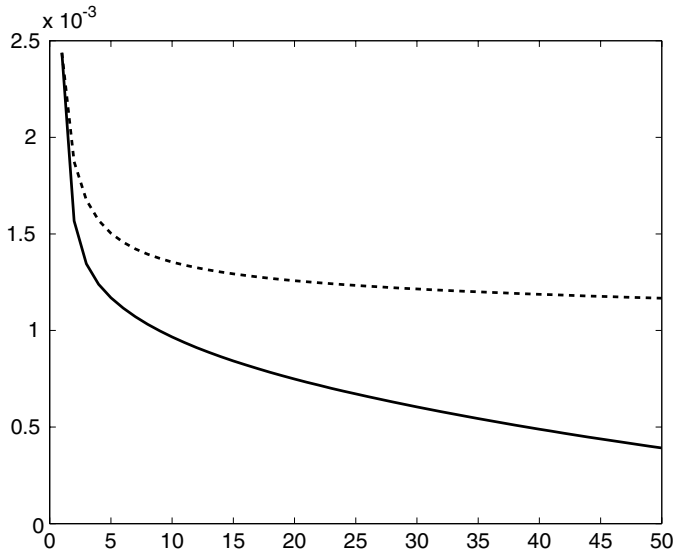

Figure 4. Convergence behaviour of the J-substitution algorithm. The dotted curve is the plot of the metric on the left side of (16) for the reconstructed conductivity image in figure 3(a) using one injection current. The full curve is the plot of the metric on the left-hand side of (20) for the reconstructed conductivity image in figure 3(b) using two injection currents. The x axis is the iteration number n.

$$\int_\Omega (\sigma_{n+1}-\sigma)\left\{\left(1+\frac{\sigma_{n+1}}{\sigma}\right)\frac{J_2^2}{\sigma_{n+1}^2}\right\}\mathrm{d}x = \int_\Omega (\sigma_{n+1/2}-\sigma)\left\{\left(1+\rho_{n+1/2}\frac{\sigma_{n+1}}{\sigma}\right)\frac{J_2^2}{\sigma_{n+1}^2}\right\}\left\{\frac{\nabla u_2^{n+1/2}\cdot(\nabla u_2^{n+1/2}+\nabla u_2)}{|\nabla u_2^{n+1/2}|(|\nabla u_2^{n+1/2}|+|\nabla u_2|)}\right\}\mathrm{d}x \tag{19}$$

and

$$\int_\Omega (\sigma_{n+1/2}-\sigma)\left\{\left(1+\frac{\sigma_{n+1/2}}{\sigma}\right)\frac{J_1^2}{\sigma_{n+1/2}^2}\right\}\mathrm{d}x = \int_\Omega (\sigma_n-\sigma)\left\{\left(1+\rho_n\frac{\sigma_{n+1/2}}{\sigma}\right)\frac{J_1^2}{\sigma_{n+1/2}^2}\right\}\left\{\frac{\nabla u_1^n\cdot(\nabla u_1^n+\nabla u_1)}{|\nabla u_1^n|(|\nabla u_1^n|+|\nabla u_1|)}\right\}\mathrm{d}x, \tag{20}$$

where $\rho_n = \frac{|\nabla u_1(\xi_0)|}{|\nabla u_1^n(\xi_0)|}$ *and* $\rho_{n+1/2} = \frac{|\nabla u_2(\xi_0)|}{|\nabla u_2^{n+1/2}(\xi_0)|}$.

Remark 3.4. Noting that

$$\frac{|\nabla u_1^n\cdot(\nabla u_1^n+\nabla u_1)|}{|\nabla u_1^n|(|\nabla u_1^n|+|\nabla u_1|)}\leqslant 1 \qquad \text{and} \qquad \frac{|\nabla u_2^{n+1/2}\cdot(\nabla u_2^{n+1/2}+\nabla u_2)|}{|\nabla u_2^{n+1/2}|(|\nabla u_2^{n+1/2}|+|\nabla u_2|)}\leqslant 1,$$

we can see that the effect of the updating process disappears if ∇u_1^n and $\nabla u_2^{n+1/2}$ have the same directions as ∇u_1 and ∇u_2, respectively and simultaneously. Therefore, to obtain a better result, we need to choose g_1 and g_2 in such a way that the angle between the generated current density vector fields $\mathbf{J}_1$ and $\mathbf{J}_2$ is bigger.

Using two injection currents shown in figures 2(b) and (c), we could reconstruct the conductivity image in figure 3(b). Compared with the reconstructed image using only one

injection current in figure 3(a), we can see that the iterative algorithm using two injection currents provides the correct image. Figure 4 shows the convergence characteristics of the J-substitution algorithm using one and two injection currents. The dotted curve is the change of the metric on the left side of (16) for the reconstructed conductivity image in figure 3(a) using one injection current. It shows that the iterative algorithm converges to a wrong image, as shown in figure 3(a). The full curve shows the change of the metric on the left side of (20) for the reconstructed conductivity image in figure 3(b) using two injection currents. As we increase the iteration number n, the iterative algorithm using two injection currents converges to the true image with a negligibly small value of the metric on the left side of (20). Various numerical experiments have been performed with simulation data and also with real experimental data in [11, 13–16].

Acknowledgments

This work was supported by grant R11-2002-103 from Korea Science and Engineering Foundation. JKS was supported in part by Korea Research Foundation KRF 2001-005-D20001.

References

[1] Alessandrini G and DiBenedetto E 1997 Determining 2-dimensional cracks in 3-dimensional bodies: uniqueness and stability *Indiana Univ. Math. J.* **46** 1–82

[2] Alessandrini G and Magnanini R 1992 The index of isolated critical points and solutions of elliptic equations in the plane *Ann. Scoula Norm. Sup. Pisa Cl Sci.* **19** 567–89

[3] Cheney M, Isaacson D and Newell J C 1999 Electrical impedance tomography *SIAM Rev.* **41** 85–101

[4] Eyuboglu E, Reddy R and Leigh J S 1998 Imaging electrical current density using nuclear magnetic resonance *Elektrik* **6** 201–14

[5] Eyuboglu M, Birgul O and Ider Y Z 2001 A dual modality system for high resolution-true conductivity imaging *ICEBI: Proc. 11th Int. Conf. on Elec. Bioimpedance (Oslo, Norway)* pp 409–13

[6] Gamba H R and Delpy D T 1998 Measurement of electrical current density distribution within the tissues of the head by magnetic resonance imaging *Med. Biol. Eng. Comput.* **36** 165–70

[7] Gamba H E, Bayford D and Holder D 1999 Measurement of electrical current density distribution in a simple head phantom with magnetic resonance imaging *Phys. Med. Biol.* **44** 281–91

[8] Ider Y Z and Birgul O 1998 Use of the magnetic field generated by the internal distribution of injected currents for electrical impedance tomography (MR-EIT) *Elektrik* **6** 215–25

[9] Joy M L G, Scott G C and Henkelman R M 1989 *In vivo* detection of applied electric currents by magnetic resonance imaging *Magn. Reson. Imaging* **7** 89–94

[10] Joy M L G, Lebedev V P and Gati J S 1999 Imaging of current density and current pathways in rabbit brain during transcranial electrostimulation *IEEE Trans. Biomed. Eng.* **46** 1139–49

[11] Khang H S, Lee B I, Oh S H, Woo E J, Lee S Y, Cho M H, Kwon O, Yoon J R and Seo J K 2002 J-substitution algorithm in magnetic resonance electrical impedance tomography (MREIT): phantom experiments for static resistivity images *IEEE Trans. Med. Imaging* **21** 695–702

[12] Kim S W, Kwon O, Seo J K and Yoon J R 2002 On a nonlinear partial differential equation arising in magnetic resonance electrical impedance tomography *SIAM J. Math. Anal.* **34** 511–26

[13] Kwon O, Woo E J, Yoon J R and Seo J K 2002 Magnetic resonance electrical impedance tomography (MREIT): simulation study of J-substitution algorithm *IEEE Trans. Biomed. Eng.* **49** 160–7

[14] Lee B I, Oh S H, Woo E J, Lee S Y, Cho M H, Kwon O, Seo J K and Baek W S 2003 Static resistivity image of a cubic saline phantom in magnetic resonance electrical impedance tomography (MREIT) *Physiol. Meas.* **24** 579–89

[15] Lee B I, Oh S H, Woo E J, Lee S Y, Cho M H, Kwon O, Seo J K, Lee J Y and Baek W S 2003 Three-dimensional forward solver and its performance analysis for magnetic resonance electrical impedance tomography (MREIT) using recessed electrodes *Phys. Med. Biol.* **48** 1971–86

[16] Oh S H, Lee B I, Woo E J, Lee S Y, Cho M H, Kwon O, Yoon J R and Seo J K 2002 Magnetic resonance electrical impedance tomography (MREIT): phantom experiments for static resistivity images using J-substitution algorithm *Proc. 2nd Joint IEEE EMBS/BMES Conf. (Houston, TX)* pp 917–8

[17] Seo J K 1996 A uniqueness results on inverse conductivity problem with two measurements *J. Fourier Anal. Appl.* **2** 515–24

[18] Scott G C, Joy M L G, Armstrong R L and Henkelman R M 1991 Measurement of nonuniform current density by magnetic resonance *IEEE Trans. Med. Imaging* **10** 362–74

[19] Scott G C, Joy M L G, Armstrong R L and Henkelman R M 1992 Sensitivity of magnetic-resonance current density imaging *J. Magn. Reson.* **97** 235–54

[20] Woo E J, Lee S Y and Mun C W 1994 Impedance tomography using internal current density distribution measured by nuclear magnetic resonance *Proc. SPIE* **2299** 377–85

[21] Zhang N 1992 Electrical impedance tomography based on current density imaging *MS Thesis* Department of Electrical Engineering, University of Toronto, Toronto, Canada